Optimization of Machining Parameters and Performance Analysis of AA2024/ZrO₂ Metal Matrix Composite Using TOPSIS: Insights into Squeeze Casting and Tribological Behavior

Ajinkya P. Edlabadkar[1], Balaji Mudadla[2], K. Karthick[3], M. Senthil Kumar[4], A. Adams[4] and Mayakannan Selvaraju[5*]

[1]Department of Mechanical Engineering, Yeshwantrao Chavan College of Engineering, Nagpur, MH, India
[2]Department of Computer Science and Engineering, CMR Technical Campus, Hyderabad, TS, India
[3]Department of Mechanical Engineering, R.M.K. Engineering College, Kavaraipettai, TN, India
[4]Centre for Material Science, Vinayaka Mission's Kirupananda Variyar Engineering College, Vinayaka Mission's Research Foundation, Salem, TN, India
[5]Department of Mechanical Engineering, Rathinam Technical Campus, Coimbatore, TN, India
*kannanarchieves@gmail.com

ABSTRACT

For the past two decades, composites have played an essential role in Engineering. A perceptive amalgamation of two or more substances yields a synergistic effect unattainable by alternative methods. Composites are materials that physically combine two or more phases to create something better than the sum of its parts. The proper selection of processing parameters is the primary determinant of the final component cast configuration. To get the best castings, the casting parameter has to be fine-tuned. In many cases, the final product features are affected by more processing parameters. Squeeze casting produces metal matrix composites; however, optimizing process parameters is necessary to achieve a superior product. Despite the significance of the applied pressure, the die and melt temperatures are the most critical process parameters affecting the outcome. Squeeze casting is effective for steel and copper alloys, cast iron, and other metals. The melting temperatures of AA2024 were investigated at 710, 740, 770, and 800 °C, and their impacts were analyzed. To investigate potential improvements in mechanical characteristics, it is vital to know whether the microstructure and particle distribution are stable after squeeze casting and whether process parameters influence the reduction of porosity. Furthermore, it investigates the response of the AA2024/nZrO₂ nanoparticles metal matrix composite to variations in melt and die temperatures, together with squeezing pressure. The two primary components of wear rate (WR) analysis for AA2024/nZrO₂ composites are assessing wear resistance and material loss during sliding. Sliding speed, load, and surface configuration are considered while calculating wear performance. Metal matrix composites made of AA2024 and nZrO₂ can have material removed using electrical discharge machining (EDM). A Technique for Order Preference by Similarity to an Ideal Solution (TOPSIS) is employed to find the optimum machining factors through the weight of entropy weight method (EWM). EDM is great at cutting complicated shapes and rigid materials. Still, it's essential to control the process parameters so the nZrO₂ nanoparticles are prevented from being damaged and the dimensions remain consistent.

Keywords: Squeeze casting; TOPSIS; AA2024; nZrO₂; Powder metallurgy.

1. INTRODUCTION

Focused on lightweight, high-strength materials, the research underscores the advancement of aluminum composites for Engineering applications, particularly improving resistance to corrosion and mechanical durability under demanding conditions (Natrayan and Kumar, 2021). The unique properties of aluminum matrix composites are affected by parameters such as reinforcement types and weight proportion, the choice of process parameters, and the matrix (Ali *et al*. 2024). The role of zirconium oxide nanoparticles in improving these properties, focusing on their potential applications in various Engineering sectors (Kumar and Irfan, 2021). The study aims to achieve specific factors like high hardness, strength, and wear resistance through effective reinforcement strategies to meet the demands of the defense, automotive, and aviation sectors (Kalaimani and Tajudeen, 2024).

The work investigates improving wear resistance in AA2024 composites with graphite reinforcement (0-10 wt%) by squeeze casting. A novel encapsulated feeding method is used to assess the tensile strength, hardness, wear properties and density of the composite (Natrayan and Kumar, 2021). The study reinforced Al6061 with varying weight percentages of Al₂O₃ nanoparticles to enhance its mechanical properties

and suitability for high-stress applications (Awate and Barve, 2021). This research examines the wear behavior of a self-lubricating hybrid composite made from AA2024, zirconia (ZrO_2) and varying graphite content(Slathia et al. 2020). The results demonstrate that the nanoscale dimensions of ZrO_2 films are affected by substrate roughness and composition, exhibiting different mechanisms for electro-assisted deposition relative to conversion coating, which leads to more uniform films on AA2024 substrates (Bonamigo *et al.* 2021).

The results highlight the enhancements in mechanical properties and overall behavior of the composites due to adding these ceramic nanoparticles (Moustafa and Taha, 2023). This work explores the superior mechanical properties of Al/(RHA+Mg+Cu) hybrid MMCs. It optimizes machining factors using Taguchi's method and Grey Rational Analysis (GRA). The results demonstrate significant improvements in hardness (35.11%), tensile strength (15.76%), and impact strength (16.67%) with rice husk ash (RHA) as a reinforcement (Muni *et al.* 2022). The research reveals that nanodiamond (ND) particles significantly reduce volumetric wear and friction coefficients at varying loads (10 N to 50 N), enhancing lubrication efficiency and minimizing energy loss during sliding (Raina *et al.* 2021). Squeeze pressure, die temperature, holding time and melting temperature were varied to correlate with hardness and tensile strength (TS), achieving a combined optimization model (Natrayan and Kumar, 2021). This study applies regression models and multi-objective optimization to improve tensile strength, elongation, and surface roughness in FSW AA2024-T3 alloy. Desirability analysis optimizes process parameters, achieving a TS of 379.69 MPa, elongation of 10.22%, and surface roughness (SR) of 6.66 HV (Boulahem *et al.* 2024).

MRR curve yields the highest material removal rate at 37.84 mm³/min, with the lowest wire wear ratio (0.0094%) at lower machining variable levels. NSGA-II optimization improves MRR by over 75%, reduces WWR by 16.50%, and improves HAMC machining (Ali *et al.* 2024). The AA2024 reinforced with Al_2O_3, ZrO_2, and graphite composites exhibited a maximum HV of 158 HV and TS of 157.36 MPa, making it suitable for various Engineering applications (Kumar and Singh, 2019). The work investigates electrical discharge machining (EDM) of Al-SiC particle-reinforced AMC using near-dry circumstances. The work material and tool are kept apart by slowly and steadily supplying a small amount of de-ionized water droplets using a minimum quantity lubrication (MQL) device (Gaigole and Rajiv, 2023). The analysis revealed that peak current is the most influential factor on MRR and SR, with optimal conditions (Ammisetti and Kruthiventi, 2024). The study evaluates AA2024 with 1.5 wt.% silicon carbide (SiC)

nanoparticles and 2 wt.% hexagonal boron nitride (h-BN) and AA2024 with two wt.% SiC and 1.5 wt.% h-BN showed significant wear only at 30°C, indicating the influence of temperature and load on the wear performance of these nanocomposites (Paulraj and Harichandran, 2020).

The SiC and seashell particle reinforcements improve tensile strength and Brinell hardness compared to base AA2024; increasing SiC from 3% to 6% reduces these properties. The 5 wt.% TiO_2 reinforcement achieves optimal hardness and wear resistance, improving hardness by 68% and wear resistance by 22% after heat treatment due to the formation of fine precipitates (Hamid *et al.* 2023). The reinforcement leads to significant grain refinement, with hardness increasing by 60% and wear resistance improving by 40 times compared to the AA2024 alloy due to better distribution of the reinforcements (Ghandourah *et al.* 2021). The tensile strength of the AA2024–AA1050 composite doubled compared to the base AA1050, and wear resistance improved by 74%, with an additional 30% enhancement from Al_2O_3 nanoparticles (Roghani *et al.* 2023). Findings indicate that S′ precipitates formed post-aging enhanced tensile strength, while the addition of alumina nanoparticles improved WR by 38% and 32% related to toughened AA1050 and AA1050/AA2024 composites, respectively (Roghani *et al.* 2024).

The ideal circumstances determined from the findings of TOPSIS and GRA were established as a spindle speed (65 m/min), a feed rate (1 mm/rev), the use of a High-Speed Steel tool, and Liquid Nitrogen coolant containing 1 wt% of nano-hexagonal boron nitride in the hybridized composite (Hariharasakthisudhan *et al.* 2024). Machining studies indicate that increasing CNT to 9% enhances SR and MRR, necessitating higher abrasive flow rates for effective material removal(Kumar and Singh, 2019). The researchers employed Taguchi's experimental design to optimize parameters including pressure, abrasive feed rate, and stand-off distance, while concurrently optimizing MRR and average roughness (Ra) with the TOPSIS methodology (Ayyandurai *et al.* 2021). The study found that the ZrO_2/graphene composite showed a significant hardness improvement (130%), while B_4C/graphene composites enhanced wear resistance by 40% compared to ZrO_2/graphene's 22% increase (Ammal and Sudha, 2023).

Studying the microstructural and tribological characteristics of AA-2024/nZrO₂ metal matrix composites within the framework of EDM is a challenging endeavor requiring careful consideration of multiple essential factors. Further research is needed to optimize the processing factors and enhance the overall efficacy of the composites' EDM. Also, understanding everything there is to consider about the mechanical and microstructural changes that happen to the composite

material is crucial. In particular, for AA2024/nZrO$_2$ MMCs, this in-depth analysis is expected to yield important insights that will help advance EDM as a strong machining method. With this newfound understanding and the backing of real-world data, AA2024/nZrO$_2$ MMCs will be used more widely in many different industries, finally realizing their full effectiveness in EDM.

2. MATERIALS AND METHODS

The AA2024 and ZrO^2 nanoparticles were commercially purchased from the Matrics enterprises, Nagercoil, Tamilnadu for this study. An internal gear mechanism in the furnace is designed to combine the molten metal with the reinforcing as the aluminum is heated in the furnace. At a speed of 200 rpm, the stirrer spins. This experimental method for making composites requires stirring the molten metal for 15 minutes prior to and after reinforcing it. The AA2024/nZrO$_2$ metal matrix composite's production process route is indicated in Fig. 1. Before the nZrO$_2$ can be dissolved into the molten metal, it is to be heated at 800 °C. The first step in casting is to bring a certain quantity of material to a molten state by adding it to the furnace. The next step is to pour the metal into an open die.
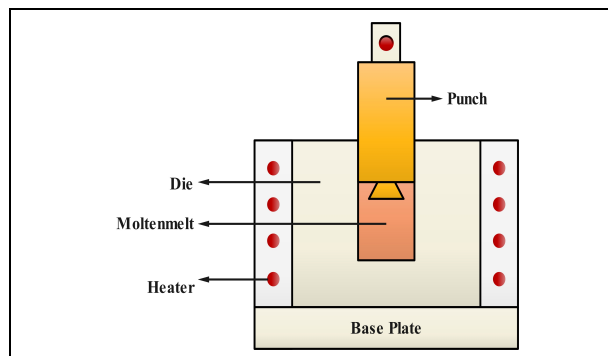
Fig. 1: An outline of fabrication using squeeze casting arrangement

During solidification, the dies exert an intensified pressure on the metals. Upon completion of the solidification process, the component is expelled. It is beneficial to apply pressure during solidification to achieve a fine-grain structure and minimize porosity formation. This study used a pressure of 80MPa in its experimental setup. Both fixed and variable parameters are present. Although the melting and die temperatures are considered to be variable, the squeezing pressure is considered to be a constant. Because aluminum hardens before the metal is transferred from the furnace to the die, a die heater is used to bring the die to a precise temperature. The volume ratio of AA2024 to nZrO$_2$is 90% to 10%. The primary applications of AA2024, a cast aluminum alloy, are sand casting and permanent mold casting. In the manufacture of MMC, it serves as a matrix metal. The experimental effort uses AA2024, a cast

metal, as a matrix metal. With less iron, the mechanical qualities of the AA2024 are improved. Table 1 displays the chemical structure of AA 2024.

Table 1. Chemical composition of AA2024

Si	Fe	Cu	Mn	Mg	Cr	Zn	Ti	Al
0.48	0.49	4.1	0.6	1.4	0.9	0.23	0.12	Bal

In this experimental work, a mixture of zirconium and oxygen, was used as reinforcement. An often-used process for making nZrO$_2$ is hot pressing. Its density is lower than that of aluminium oxide. It sublimes at about 2700°C after undergoing allotropic phase transitions above 2000°C. Alpha zirconium dioxide has a hexagonal structure, while beta zirconium dioxide is cubical. Using rotation speeds of 1000 and 1200 rpm, the study found that the incorporation of nZrO$_2$ nanoparticles led to a microhardness increase of up to 48% and a wear rate (WR) decrease of 62% related to the AA7075, benefiting from refined microstructures and improved hardness (HV) and wear properties(Jamali and Mirsalehi 2022). Hardness levels of nZrO$_2$ abrasives range from F1500 to F360. F320 is utilized in this experimental study. The samples were prepared according to the method parameters, as shown in Table 2.

Table. 2 Processing Criteria

AA2024 Temperature (ºC)	Mold temperature (ºC)
(710, 740, 770, 800)	340

AA2024/nZrO2 metal matrix composites (MMCs) outperform conventional metals in mechanical strength, thermal stability, and wear resistance. The incorporation of nZrO2 particles significantly enhances tensile strength, hardness, and stiffness, making these composites more resistant to deformation compared to traditional aluminum or steel. Their superior thermal conductivity and lower thermal expansion improve heat dissipation and minimize distortion under high temperatures, making them suitable for aerospace and automotive applications. Additionally, the presence of nZrO2 reinforcement greatly increases wear resistance, reducing material loss in abrasive conditions. These combined advantages make AA2024/nZrO2 MMCs a preferred choice for high-performance engineering applications where strength, durability, and thermal efficiency are critical.

3. RESULTS AND DISCUSSION

3.1 Impact of Ultimate Tensile Strength (UTS)

Fig. 2 shows the tensile strength values of the composite material made of AA2024 and nZrO$_2$. The tensile testing specimen was prepared according to the guidelines laid out by ASTM D3039. The wire-cut EDM technique is used to first section the squeeze cast

specimen AA2024/nZrO$_2$ metal matrix composite into appropriate dimensions. So that the tensile test is carried out, the composite is made in line with the dog bone shape. The tensile test was conducted on six of the eight produced samples. Because a lower melt temperature might result in a finer grain structure and an increased grain size from a slower cooling rate, an increase in melt temperature significantly lowers the UTS of the AA2024-nZrO$_2$. Grain size determines the tensile characteristics of the Squeeze Casting sample; lower tensile strength is usually the result of coarse grain structure, and higher tensile strength is the result of fine grain structure (Chang *et al.* 2021). Increases in percentage elongation and final tensile strength result from a faster cooling rate. Grain size determines the tensile qualities of Squeeze Casting; toughness and ductility are enhanced with fine grain structure, but strength and ductility are reduced with coarse grain structure. Crack resistance and fatigue endurance are better with coarse grain structure. The composite AA2024/nZrO$_2$ exhibits a bimodal microstructure and demonstrates improved mechanical properties, achieving a tensile strength (TS) of 382 MPa and an elongation of 16%, with further T6 heat treatment boosting strength to 624 MPa but reducing ductility to 5.6% (Wei *et al.* 2024).
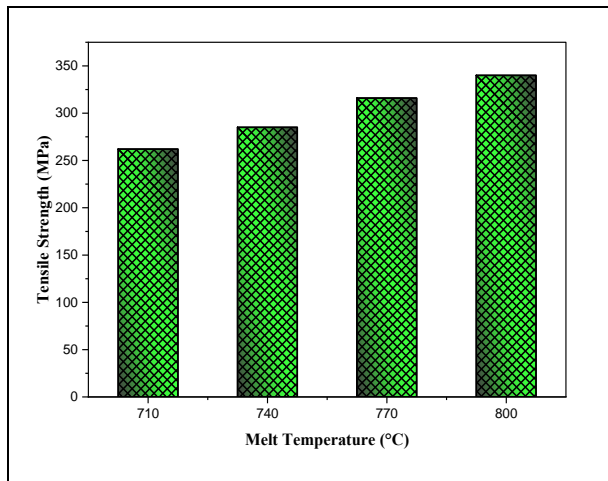

Fig. 2: Evaluation of UTS of AA 2024/nZrO$_2$ composite

3.2 Impact of Hardness

Scratch, rebound, and indentation hardness are the three main operational definitions of hardness in materials research. Using Vickers hardness measurements, this experiment examined that nZrO$_2$ reinforcement altered the distribution and characteristics of aluminum alloy. The Vickers hardness test is the most widely used and recognized hardness test for all metals. Particles of zirconium dioxide are evenly spaced along the whole specimen. Preparing the specimen for the Vickers micro-hardness test involves steps such as polishing it using 800 grade Emery sheet. The hardness is highly sensitive to the temperature of the prepared die. Raising the die temperature causes the grains to be larger

because heat transfers are slower and the mold and die cool at different rates.

The hardness value drops as the melt temperature rises (Fig. 3), as the cooling rate becomes noticeably slower. Melt temperatures of 780 °C have a more excellent Vickers hardness value than those at 740 °C and 800 °C, respectively. The nanocomposite with 5 wt% nZrO$_2$ achieved maximum hardness (124.5 BHN), TS (88.9 MPa), and wear resistance (9.802 mm^3/m at 20 N), while the 3 wt% nZrO$_2$ exhibited the highest impact strength (22.8 J/mm^2) (Chandradass *et al.* 2023).
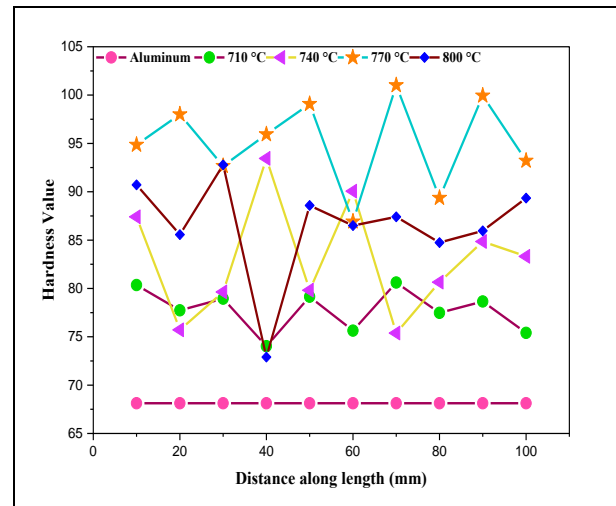

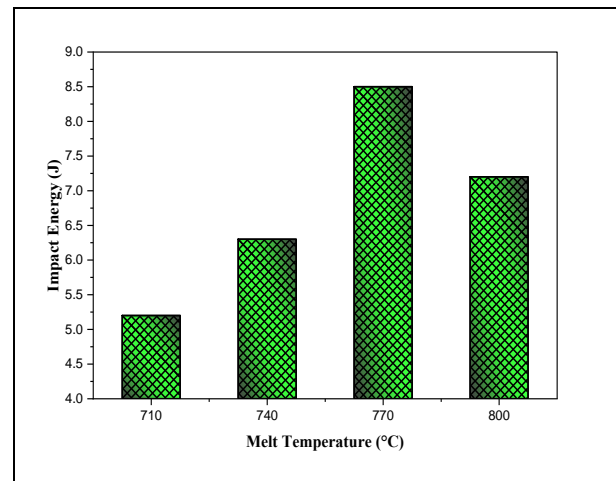**Fig. 3: Evaluation of hardness of AA2024/nZrO$_2$ composite**

**Fig. 4: Evaluation of impact energy AA2024/nZrO$_2$ composite**

3.3 Impact on Impact Energy

Fig. 4 illustrates the impact energy values of the AA2024/nZrO$_2$ metal matrix composite. The absorbed energy quantifies the material's toughness and is contingent upon the reinforcement volume. Consistency is maintained in this metal matrix, comprising 90% AA2024 and 10% nZrO$_2$. An elevated impact value is

achieved at increased melt temperatures due to thermal expansion between the reinforcing and matrix materials. Results show that 2.5 wt.% TiO_2 with AA2024 enhances grain morphology, increases impact strength from 5 to 7 J/m², and improves wear resistance, with maximum hardness at 5 wt.% TiO_2 (Hamid *et al.* 2023).
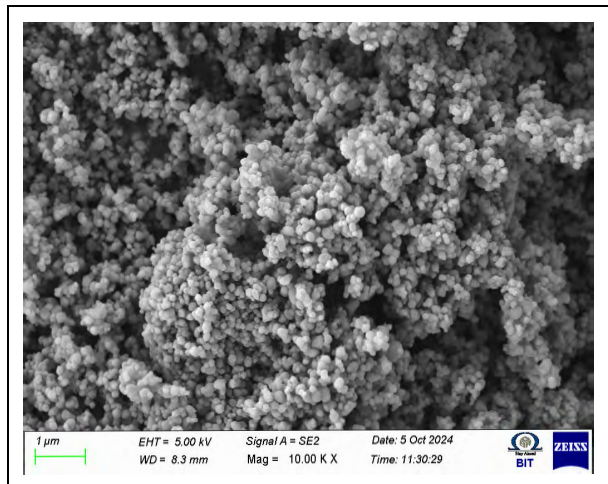
Fig. 5: SEM image of ZrO_2 nanoparticles at 710°C melting temperature (10.00 KX)
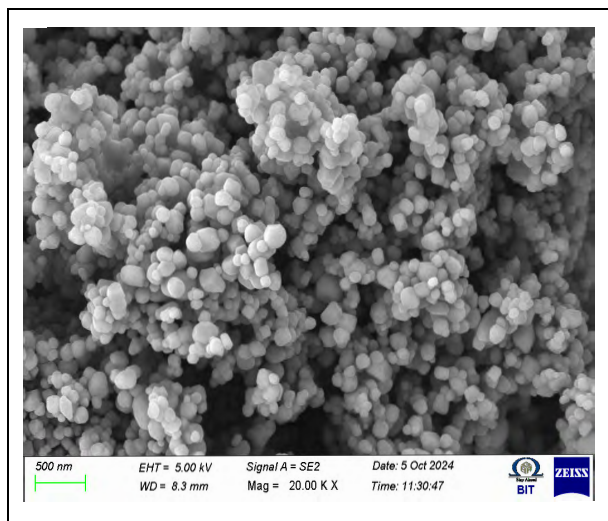
Fig. 6: SEM image of $nZrO_2$ nanoparticles at 20.00 KX magnification

3.4 Scanning Electron microscopic Analysis

The volume fraction of zirconium dioxide particles is determined using ZEISS in compliance with ASTM E766 standards. Fig. 5 indicates that nanoparticles of ZrO_2 are melting at a melting point of 710°C. Because the melt temperature is higher than the reinforcement temperature, it is finely distributed at 770°C (Fig. 6). Particles of zirconium dioxide and AA2024 appear as fused black particles in the 10.00KX micrograph of the sintered and compressed matrix. Due to its increased addition, the sintered aluminum alloy

matrix contains a higher concentration of composite $nZrO_2$. No empty spaces were observed in the mixture of the composite particles and the grains. The research examines the FSW of dissimilar AA6061 and AA2024 alloys using varying rotational speeds and tool geometries. SEM analyses reveal optimal tensile properties at 900 rpm, while a hardness of 112 HV is obtained at 1120 rpm(Santhosh Kumar et al. 2020). Fig. 6 presents a micrograph of the identical sintered sample with 10% zirconium dioxide within the AA 2024 matrix. With a magnification of 20.00KX, the grain boundaries containing composite particles and eutectic components have been seen. Between the interlocking grains, the matrix shows no signs of holes.

Analyzing the surface morphology and microstructure of an AA-2024/$nZrO_2$ Metal Matrix Composite (MMC) using Scanning Electron Microscopy (SEM) is all about in these works. This research sheds insight into many microstructural features, including the distribution of $nZrO_2$ inside the AA2024 matrix and the stability of the matrix-reinforcement contact. Scanning electron microscopy can show the AA2024/$nZrO_2$ MMC's intricate microstructure. The $nZrO_2$ embedded in an aluminum matrix can be studied in size, shape, and dispersion. The microstructure may be a combination of dendritic aluminum grains and $nZrO_2$ nanoparticles.

The $nZrO_2$ dispersion can be better assessed with scanning electron microscopy (SEM) images at different magnifications. It is best to have a uniformly dispersed arrangement to improve mechanical qualities. As seen in Fig. 7 (a-d), particle aggregation can also be seen, which affects the mechanical performance. It is possible to evaluate the interfacial quality of the $nZrO_2$ nanoparticles and the aluminium matrix. A well-defined interface shows adequate wetting and adhesion between the reinforcement and matrix. Delamination, cracks, or holes at the interface suggest a lack of proper adhesion. Scanning electron micrographs (SEMs) shed light on the nature of the link between the $nZrO_2$ nanoparticles and the aluminum matrix. Very little debonding or particle extraction upon fracture would indicate a strong connection. Debonding and pull-out of particles can occur due to inadequate bonding, reducing mechanical characteristics. Scanning electron microscopy (SEM) detects internal composite flaws like porosity and voids. These attributes influence the mechanical strength and integrity of the material. SEM images show that grains' structure, size, and alignment can impact the composite's mechanical characteristics. SEM is instrumental in understanding the composite's failure mechanisms, particularly when examining fracture surfaces. This method allows for analysis of how ZrO_2 nanoparticles affect crack initiation, propagation, and the fracture mode (e.g., ductile or brittle). Additionally, when combined with SEM, EDS enables elemental analysis across various locations, confirming the presence and spatial distribution of aluminum and zirconium dioxide phases.

The SR of the specimen, which is crucial for considerate wear behavior and tactile interactions, was clearly shown by SEM images. Following fatigue testing, SEM analysis provided a detailed view of crack initiation and progression, shedding light on how the material responds under fatigue conditions.
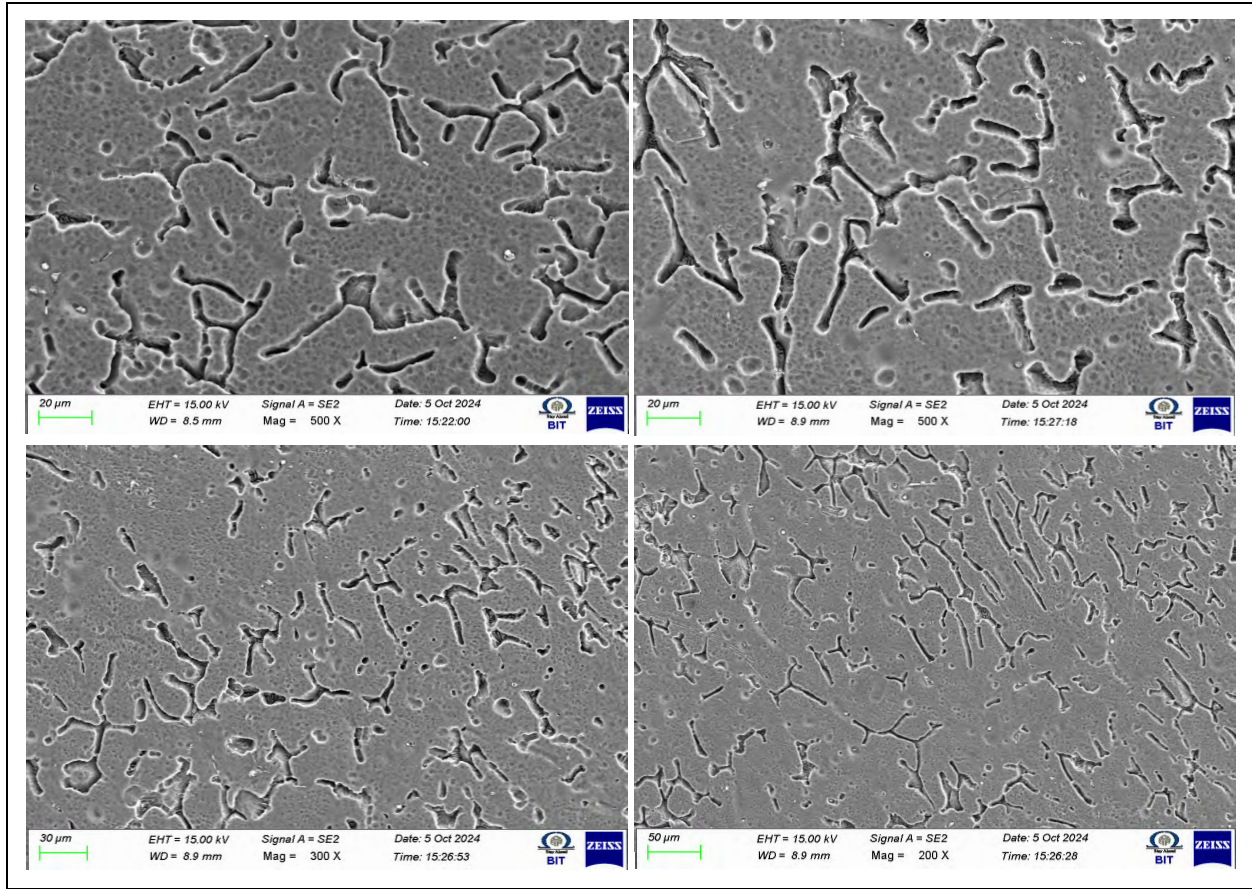

Fig. 7: (a-d) SEM image of AA2024/nZrO$_2$ composites

Table. 3 Comparison of WR (mm^3/km) under a continuous load of 50 N at several temperatures

Temperature (°C)	AA2024	AA2024/nZrO$_2$
710	1.03	0.95
740	1.21	1.16
770	1.46	1.41
800	1.77	1.62

3.5. Analysis of Specific Wear Rate

The AA-2024/nZrO$_2$ metal matrix composite wear rate study examines the rate at which a particular substance deteriorates or becomes degraded due to sliding/abrasive contact with each other. A pin-on-disc tribometer is utilized for WR analysis. Sliding the AA2024/nZrO$_2$ composite sample against a counter-face material (such as steel or ceramic) applies regulated stress once it is formed in the proper geometry. As wear progresses, the tribometer analyzes the resulting frictional forces. The WR of the sample was determined using the given formula (Table 3).

$$WR = \frac{\text{volume (V)}}{\text{load (P)} \times \text{Sliding distance (s)}} \qquad \ldots (1)$$

The wear rate study comprises experimenting with different loads and sliding velocities to determine which factors affect the wear properties of the composites. The assessment of wear characteristics under various working conditions is made possible by varying mixtures of loads and sliding velocity. Metal matrix composites AA-2024/nZrO$_2$ are susceptible to adhesive, abrasive, and delamination wear as their wear mechanisms. Results indicate that 9 wt% of reinforcement with AA2024 using squeeze casting improves hardness, tensile, and compressive strength, while reducing wear rate by forming a protective layer. Adhesive wear arises from localized welding and subsequent material detachment. In contrast, abrasive wear is caused by the erosion of the opposing surface by hard nZrO$_2$ nanoparticles (Fig. 8). The delamination of composite layers causes wear. The AA-2024/nZrO$_2$ composite's worn surface is examined using scanning electron microscopy (SEM) and other techniques once the wear testing is completed as illustrated in Fig. 9.

Researchers observe that the wear rate varies with different amounts of $nZrO_2$ in the composite, impacting the composite's mechanical characteristics and WR. A consistent dispersion of $nZrO_2$ is often chosen to improve WR. To obtain the comparative wear performance of AA-2024/$nZrO_2$ MMC, the wear rate was compared to that of other materials, like the base alloy. An outcome of the WR study is vital for improving the application of AA-2024/$nZrO_2$ in various technical disciplines where wear resistance is of the utmost importance, such as aerospace parts, automotive components, and high-performance machinery.
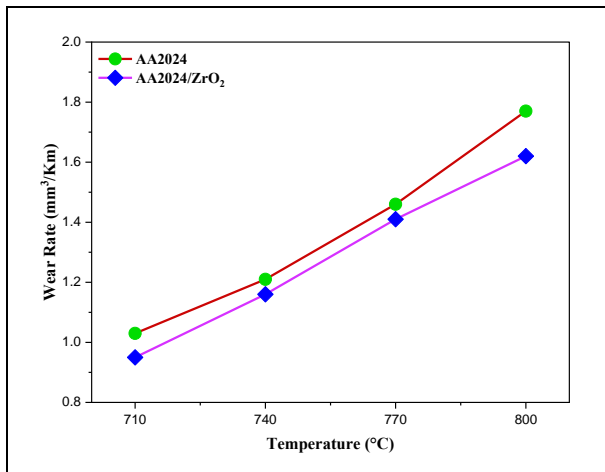

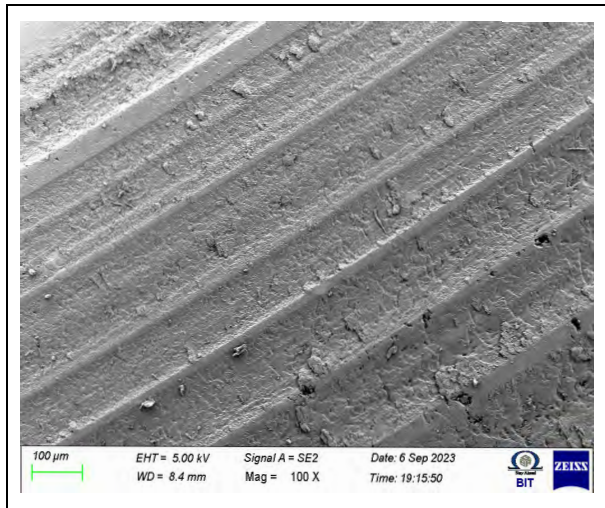Fig. 8: Evaluation of wear rate at different temperatures

Fig. 9: SEM image of WR analysis

3.6. Machinability

Machinability refers to the extent to which a material can be easily machined. This attribute is intricate and contingent upon various aspects, including the material's hardness, machinability, and stiffness. The AA2024/$nZrO_2$MMC comprises AA2024 and $nZrO_2$ particles. The $nZrO_2$ nanoparticles enhance the strength, stiffness, and wear resistance of the composite; yet, they

complicate the machining process. The machinability of the AA2024/$nZrO_2$MMC is typically regarded as inferior to that of the AA2024. The abrasiveness of the composite is augmented by the ZrO_2 nanoparticles, potentially resulting in heightened tool wear and surface irregularities. Moreover, the enhanced strength of the composite complicates the material removal process (Fig. 10).

Fig. 10: EDM operation

Table 4. Input levels of the processing factor

Processing factor	Notation	Unit	Level		
			1	2	3
Current gap	A	ampere	5	8	11
Ton	B	μs	3	6	9
Toff	C	μs	2	5	8

Table. 5 Experimental designs of the current analysis

Exp. No.	A	B	C	MRR mm³/min	Surface Roughness μm	Machining Time min
1	5	3	2	0.017	5.25	30
2	8	3	5	0.028	5.77	26
3	11	3	8	0.033	7.56	19
4	8	6	2	0.036	7.93	22
5	11	6	5	0.027	4.35	29
6	5	6	8	0.023	4.75	28
7	11	9	2	0.040	6.54	18
8	5	9	5	0.029	5.98	27
9	8	9	8	0.034	6.9	21

Various parameters influence the composite, such as the $nZrO_2$ concentration, particulate size, matrix alloy, and machining conditions. Generally, an increased $nZrO_2$ content correlates with greater machining difficulty of the composite. Reduced particle sizes additionally complicate the machining of the composite. The matrix alloy can influence machinability, as certain

alloys exhibit superior machinability compared to others. The machining factors, including cutting speed, and tool material, feed rate, significantly influence machinability (Tables 4 and 5).

The AA2024/nZrO₂ composite material can be effectively molded and refined using EDM. Increased strength, rigidity, and WR are the superior mechanical properties of this composite compared to the underlying aluminum alloy. This work concentrates on optimizing wire-cut EDM parameters such as pulse ON-Time, gap voltage, and pulse OFF-Time, during the machining of nano-SiC and nano-nZrO₂ reinforced in an AA6061 aluminum alloy matrixcomposite (Thiagarajan *et al.* 2023).

In electrical discharge machining (EDM), the tool electrode and the workpiece electrode produce high-frequency electrical discharges. The dielectric fluid removes the minute particulates from the workpiece material, which are evaporated and dissolved by the discharges. The EDM parameters are adjusted to regulate the procedure. A heat-affected zone surrounds the machined elements because EDM can produce heat during the machining process. Nanoparticles of zirconium dioxide ($nZrO_2$) act as heat absorbers in AA-2024/nZrO₂, reducing the HAZ and enhancing heat dissipation. This property is advantageous because it mitigates the impact of heat on the composite material's properties. It is possible to achieve complex geometries and exceptional precision with EDM. However, the spark erosion procedure produces a unique roughness in the surface finish. If necessary, post-machining techniques such as grinding or polishing can be implemented to improve the surface quality.

4. MULTI-OBJECTIVE OPTIMIZATION TECHNIQUE

4.1 Entropy Weight Measurement (EWM) Technique

The index weight is determined through the application of the EWM procedure in this investigation. The entropy weight technique mechanically solves mathematical models to assess weights based on the quantity of information, disregarding the decision maker's input. The weightage index for each machining characteristic is determined using the following methods (Dhilip *et al.* 2024).

Step 1: The preliminary step involves assessing 'm' alternatives based on 'n' attributes, where the alternatives consist of process factors such as Gap Current, Ton, and Toff, while the attributes represent response parameters including MRR, Surface Roughness, and Machining Time for this specific issue.

Step 2: The initial findings are transformed into a decision matrix denoted as $D[x_{ij}]_{m \times n}$ where m denotes the number of possibilities, n signifies the number of attributes, and x_{ij} represents the value of the jth attribute for the ith factor.

$$Q_{ij} = \frac{r_{ij}}{\sum_{i=1}^{m} r_{ij}} \qquad \dots (2)$$

Step 3: The choice matrix is normalized by favorable attributes (i.e., max) and non-beneficial attributes (i.e., min) to relate the response factors. The mathematical equation that follows can be used to calculate the normalized matrix.

$$e_j = -\frac{1}{\ln m} \sum_{i=1}^{m} \left(\frac{r_{ij}}{\sum_{i=1}^{m} r_{ij}} \right) \ln \left(\frac{r_{ij}}{\sum_{i=1}^{m} r_{ij}} \right) \qquad \dots (3)$$

Step 4: Compute the entropy value ' e_j ' which signifies the assessment of the jth index.

Step 5: $EWM(w_j)$ of the jth index is evaluated (Mohankumar *et al.* 2024).

$$w_j = \frac{1 - e_j}{n - \sum_{j=1}^{n} e_{ij}} \qquad \dots (4)$$

Table 6. Weightage of each response

	MRR	**SR**	**Machining Time**
Wj	0.437	0.304	0.259

4.2 TOPSIS

Hwang and Yoon introduced the TOPSIS in 1981. This mathematical method integrates the weights of machining parameters according to the decision maker's preferences to resolve multi-objective issues and achieve a singular optimal solution. This method broadly applies to all suitable practical methods for achieving a viable, faultless solution. The rational approach of the positive and negative ideal solution is characterized by all experimental results being within the defined limits of maximum and minimum, resulting in satisfactory outcomes. The TOPSIS multi-objective optimization identifies optimal processing parameters, establishing the most influential settings for improved mechanical properties (Purusothaman *et al.* 2021).

The main objective is to delineate the viable solution and evaluate the model by computing the closeness coefficient between the actual and optimal solutions. The TOPSIS approach is succinctly described below.

Step 1: The decision matrix is normalized by employing the subsequent equation.

$$T_{ij} = \frac{x_{ij}}{\sqrt{\sum_{i=1}^{m} x_{ij}^2}} \qquad \dots (5)$$

Whereas $i = 1, 2, \ldots \ldots m$; $j = 1, 2, \ldots \ldots n x_{ij}$ denotes the actual value of the ith value of the jth experimental run and T_{ij} the equivalent normalized value.

Step 2: The entropy weight measurement method is employed to ascertain the weighted matrix for each result.

Step 3: The normalization matrix is multiplied by the corresponding weights obtained using the entropy weight technique to yield the weightage normalized decision matrix. The following equation determines the weighted normalized decision matrix (Bhaskar *et al.* 2013).

$$V_{ij} = w_i \times T_{ij} \qquad \ldots (6)$$

whereas w_j denotes the weightage of the jth attribute. The Normalized Decision Matrix done using weight is derived using equations (5) and (6), as seen in Table 7.

Step 4: The weighted choice matrix is employed to establish the negative (V^-) and the positive (V^+) ideal solution for the suboptimal, and optimal value, respectively.

$$V^+ = (V_1^+, V_2^+, \cdots \cdots V_n^+)\text{Max} \qquad \ldots (7)$$

$$V^- = (V_1^-, V_2^-, \cdots \cdots V_n^-)\text{Min} \qquad \ldots (8)$$

Step 5: The separation distance of each viable solution is computed using the following equation (table 8).

$$S_i^+ = \sqrt{\sum_{j=1}^{n} \left(V_{ij} - V_j^+\right)^2} \qquad \ldots (9)$$

$$S_i^- = \sqrt{\sum_{j=1}^{n} \left(V_{ij} - V_j^-\right)^2} \qquad \ldots (10)$$

Step 6: The relative closeness coefficient (P_i) to the ideal solution is calculated according to the equation.

$$P_i = \frac{S_i^-}{S_t^+ + S_i^-} \qquad \ldots (11)$$

Step 7: Order ranking of the system (Karthikraja *et al.* 2024).

The closeness-coefficient value is used to organize alternative data collection in ascending order (Table 8).

Table 7. Normalize matrix and weightage of each response

Experiment No.	Normalized Data			Weighted Data		
	MRR	SR	Machining Time	MRR	SR	Machining Time
1	0.1865	0.2908	0.4350	0.0815	0.0883	0.1128
2	0.3071	0.3196	0.3770	0.1342	0.0970	0.0978
3	0.3619	0.4187	0.2755	0.1582	0.1271	0.0715
4	0.3948	0.4392	0.3190	0.1726	0.1333	0.0827
5	0.2961	0.2409	0.4205	0.1294	0.0731	0.1091
6	0.2523	0.2631	0.4060	0.1103	0.0799	0.1053
7	0.4387	0.3622	0.2610	0.1917	0.1100	0.0677
8	0.3181	0.3312	0.3915	0.1390	0.1006	0.1015
9	0.3729	0.3822	0.3045	0.1630	0.1160	0.0790
			V+	0.1917	0.0731	0.0677
			V-	0.0815	0.1333	0.1128

Table 8. The Ranking order of the matrix

Separation Matrix		Closeness- coefficients	Rank
Si+	Si-	Pi	
0.1201	0.0451	0.2729	9
0.0692	0.0658	0.4874	7
0.0637	0.0874	0.5784	4
0.0649	0.0959	0.5963	3
0.0748	0.0770	0.5074	5
0.0900	0.0612	0.4047	8
0.0368	0.1214	0.7673	1
0.0684	0.0672	0.4955	6
0.0529	0.0899	0.6298	2

Table 9. The optimum result of the machining factor

Exp. No.	A	B	C	MRR	SR	Machining Time
7	11	9	2	0.04	6.54	18

This employs a combined approach of EWM and TOPSIS to optimize the machining features of AA2024–nZrO$_2$ composite materials during the Squeeze Casting Method. This integrated method employs computational procedures to assess and rank the optimal machining features for the selected model. The weighted normalized decision matrix is computed using equations (2) to (4) for each member within the matrix (Step 3). The matrix's weight is presented in Table 6. It is noticed that

a greater entropy weight of the index is more beneficial than a lower value. The closeness coefficients are ordered based on their relative significance. A superior CCo number signifies the ideal combination of qualities relative to others. The parameter configuration of the seventh experiment is the most effective machining, as indicated by the final matrix of Table 8. The ongoing investigation is deemed to be in significant agreement. The ideal arrangement of machine parameters is outlined below (Table 9).

5. CONCLUSION

The AA2024/nZrO$_2$MMC was fabricated and its characteristics were assessed through tensile testing, hardness testing, impact testing, and microstructural analysis.

- The improved melt temperature negatively impacts the UTS of AA2024/nZrO$_2$ squeeze casting components at 800°C because of a reduced cooling rate. The MMC's ductility decreases at high temperatures.

- Experimental findings demonstrate that the increased melting temperature of 800°C reduces hardness and impact value. The material has less plastic deformation at high temperatures. The temperature of 770°C unequivocally signifies enhanced particle dispersal and the necessary thermal threshold.

- The nZrO$_2$ cluster is produced at a melting temperature of 710°C and is uniformly dispersed at 770°C, which is optimum for sample processing under a pressure of 80 MPa.

- The AA2024/nZrO$_2$ metal matrix composite exhibited much better wear resistance than the base alloy in the wear rate examination. Under different working conditions, adding nZrO2 nanoparticles significantly improved the composite's mechanical characteristics, leading to a decrease in wear rates.

- The study emphasizes the possibility of using AA2024/nZrO$_2$ composites in industries with severe wear, such as aerospace and automotive. Additional investigation into the composite's tribological and microstructural characteristics yields valuable information for enhancing its performance and making it usable in the real world.

- More investigation is required into the potential of the AA2024/nZrO$_2$ composite as a long-lasting and dependable material for use in environments prone to wear.

A new class of materials called AA2024/nZrO$_2$ metal matrix composites has emerged, showing improved mechanical, thermal, and wear characteristics over conventional metals. Much study has been done on their processing, characteristics, and uses. Future technical developments and problem-solving should lead to AA2024/nZrO$_2$ composites finding more uses in various engineering fields.

Despite all their benefits, interfacial bonding, reinforcement particle agglomeration, and the high cost of nZrO$_2$ nanoparticles are still problems that need fixing in AA2024/nZrO$_2$composites. To expand their broad applicability, future research should focus on improving processing methods and refining the characteristics of these composites. This investigation will examine the material's porosity, density, and grain size. Researchers intend to use modeling and finite element software for analytical tasks.

Experimental techniques such as advanced microscopy (TEM, AFM) for microstructural analysis or high-speed thermal imaging for real-time machining insights could provide deeper understanding. Alternative reinforcements like graphene, carbon nanotubes, or B$_4$C may enhance mechanical, thermal, and wear properties beyond SiC. Additionally, investigating hybrid composites with multi-reinforcement systems and exploring alternative machining processes like laser-assisted or ultrasonic machining could optimize performance for specialized applications.

FUNDING

CONFLICTS OF INTEREST

The authors declare that there is no conflict of interest.

COPYRIGHT

REFERENCES

Ali, M. A., Mufti, N. A., Ishfaq, K., Naveed, R., Saleem, M. Q. and Qureshi, A. M., Development and characterization of hybrid aluminium matrix composites through stir-squeeze casting using distinct reinforcements for structural applications, *Int. J. Adv. Manuf. Technol.*, 133(11–12), 5897–5925 (2024).
https://doi.org/10.1007/s00170-024-14102-9

Ammal, M. A. and Sudha, J., Microstructural Evolution & Mechanical Properties of ZrO_2 /GNP and B_4 C/GNP reinforced AA6061 Friction Stir Processed Surface Composites - A Comparative study, *Proc. Inst. Mech. Eng., Part B: J. Eng. Manuf.*, 237(8), 1149–1160 (2023).
https://doi.org/10.1177/09544054221126942

Ammisetti, D. K. and Kruthiventi, S. S. H., Experimental Analysis and Artificial Neural Network Teaching–Learning-Based Optimization Modeling on Electrical Discharge Machining Characteristics of AZ91 Composites, *J. of Materi. Eng. and Perform.*, 33(21), 11718–11735 (2024).
https://doi.org/10.1007/s11665-023-08795-4

Awate, P. P. and Barve, S. B., TOPSIS & EXPROM2 multicriteria decision methods for Al2O3/Al 6061 nanocomposite selection, *Mater. Today Proc.*, 468352–8358 (2021).
https://doi.org/10.1016/j.matpr.2021.03.402

Ayyandurai, M., Mohan, B. and Anbuchezhiyan, G., Characterization and machining studies of nano borosilicate particles reinforced aluminium alloy composites using AWJM process, *J. Mater. Res. Technol.*, 152170–2187 (2021).
https://doi.org/10.1016/j.jmrt.2021.09.014

Bhaskar, K., Nagarajan, G. and Sampath, S., Optimization of FOME (fish oil methyl esters) blend and EGR (exhaust gas recirculation) for simultaneous control of NOx and particulate matter emissions in diesel engines, *Energy*, 62224–234 (2013).
https://doi.org/10.1016/j.energy.2013.09.056

Bonamigo, M. V., Puiggalí-Jou, A., Jiménez-Piqué, E., Alemán, C., Meneguzzi, A. and Armelin, E., Green Nanocoatings Based on the Deposition of Zirconium Oxide: The Role of the Substrate, *Materials*, 14(4), 1043 (2021).
https://doi.org/10.3390/ma14041043

Boulahem, K., Salem, S. B., Shiri, S. and Bessrour, J., Experimental Modeling and Multi-Response Optimization in Friction Stir Welding Process Parameters of AA2024-T3 Using Response Surface Methodology and Desirability Approach, *Exp. Tech.*, 48(5), 833–849 (2024).
https://doi.org/10.1007/s40799-023-00691-9

Chandradass, J., Thirugnanasambandham, T. R. R. and Palanivendhan, M., Effect of ZrO_2 Nanoparticles Loading on the Tribo-Mechanical Behavior of Magnesium Alloy Nanocomposites, *SAE Tech. Paper*, 2023-28–0130 (2023).
https://doi.org/10.4271/2023-28-0130

Chang, X., Chen, G., Sun, W., Zhang, H., Chu, G., Zhang, X. and Du, Z. (2021). Microstructures, mechanical properties and solidification mechanism of a hot tearing sensitive aluminum alloy asymmetric part fabricated by squeeze casting. Journal of Alloys and Compounds, 886, 161254.
https://doi.org/10.1016/j.jallcom.2021.161254

Dhilip, J. D. J., Ganesan, K. P. and Sivalingam, V., Machinability Studies and Optimization of Process Parameters in Wire Electrical Discharge Machining of Aluminum Hybrid Composites by the VIKOR Method, *J. of Materi. Eng. and Perform.*, 33(11), 5547–5562 (2024).
https://doi.org/10.1007/s11665-023-08323-4

Gaigole, P. M. and Rajiv, B., Multi-performance characteristics optimization in near-dry rotary EDM of AlSiC by weighted principal component analysis, *Mater. Today Proc.*, S2214785323011185 (2023).
https://doi.org/10.1016/j.matpr.2023.03.075

Ghandourah, E. I., Moustafa, E. B., Hussein, H. and Mosleh, A. O., The Effect of Incorporating Ceramic Particles with Different Morphologies on the Microstructure, Mechanical and Tribological Behavior of Hybrid TaC_ BN/AA2024 Nanocomposites, *Coatings*, 11(12), 1560 (2021).
https://doi.org/10.3390/coatings11121560

Hamid, M. Mahan., S. V. Konovalov, Irina, P. and Mudhar, A. A. O., The Effects of Titanium Dioxide (TiO2) Content on the Dry Sliding Behaviour of AA2024 Aluminium Composite, *J. Mech. Eng.*, 20(3), 239–261 (2023).
https://doi.org/10.24191/jmeche.v20i3.23910

Hariharasakthisudhan, P., Logesh, K., Sathish, K., Sivakumar, R. and Sathickbasha, K., Optimizing the drilling process parameters of AZ91 based hybrid composites using TOPSIS and grey relational analysis, *Eng. Res. Express*, 6(3), 035559 (2024).
https://doi.org/10.1088/2631-8695/ad72cd

Jamali, A. and Mirsalehi, S. E., Production of AA7075/ZrO2 nanocomposite using friction stir processing: Metallurgical structure, mechanical properties and wear behavior, *CIRP J. Manuf. Sci. Technol.*, 3755–69 (2022).
https://doi.org/10.1016/j.cirpj.2021.12.008

Kalaimani, M. and Tajudeen, S., Investigation of Wear Performance in Zirconium Dioxide Reinforced Aluminum Hybrid Nanocomposites Synthesized by the Powder Metallurgy Process. *SAE Tech. Paper,* 2023-01–5161 (2024).
https://doi.org/10.4271/2023-01-5161

Kumar, N. and Irfan, G., A review on tribological behaviour and mechanical properties of Al/ZrO2 metal matrix nano composites, *Mater. Today Proc.*, 382649–2657 (2021).
https://doi.org/10.1016/j.matpr.2020.08.240

Kumar, R. and Singh, M., Experimental Investigation of Performance and Emission characteristics of DI CI Engine with Dual Biodiesel Blends of Mexicana Argemone and Mahua, *Mater. Today Proc.*, 16321–328 (2019).
https://doi.org/10.1016/j.matpr.2019.05.097

Mohankumar, V., Kumarasamy, S. P., Palanisamy, S., Kuriakose, M. A., Durairaj, T. K., Sillanpää, M. and Al-Farraj, S. A., Process parameters optimization of EDM for hybrid aluminum MMC using hybrid optimization technique, *Heliyon*, 10(15), e35555 (2024).
https://doi.org/10.1016/j.heliyon.2024.e35555

Moustafa, E. B. and Taha, M. A., The Effect of Mono and Hybrid Additives of Ceramic Nanoparticles on the Tribological Behavior and Mechanical Characteristics of an Al-Based Composite Matrix Produced by Friction Stir Processing, *Nanomaterials*, 13(14), 2148 (2023). https://doi.org/10.3390/nano13142148

Muni, R. N., Singh, J., Kumar, V., Sharma, S., Sudhakara, P., Aggarwal, V. and Rajkumar, S., Multiobjective Optimization of EDM Parameters for Rice Husk Ash/Cu/Mg-Reinforced Hybrid Al-0.7Fe-0.6Si-0.375Cr-0.25Zn Metal Matrix Nanocomposites for Engineering Applications: Fabrication and Morphological Analysis, *J. Nanomater.*, 2022(1), 2188705 (2022). https://doi.org/10.1155/2022/2188705

Natrayan, L. and Kumar, M. S., Optimization of wear parameters of aluminium hybrid metal matrix composites by squeeze casting using Taguchi and artificial neural network, *Manuf. and Des.*, Elsevier, 223–234 (2021)., https://doi.org/10.1016/B978-0-12-822124-2.00010-X

Paulraj, P. and Harichandran, R., The tribological behavior of hybrid aluminum alloy nanocomposites at High temperature: Role of nanoparticles, *J. Mater. Res. Technol.*, 9(5), 11517–11530 (2020). https://doi.org/10.1016/j.jmrt.2020.08.044

Purusothaman, M., Rajesh, S. and Chokkalingam, R., TOPSIS multiobjective optimization of powder metallurgy process parameters: Al-NiTi-SiC smart composites, *Mater. Today Proc.*, 456907–6910 (2021). https://doi.org/10.1016/j.matpr.2021.01.026

Raina, A., Irfan. U. Haq, M., Anand, A., Mohan, S., Kumar, R., Jayalakshmi, S. and Arvind, S., R., Nanodiamond Particles as Secondary Additive for Polyalphaolefin Oil Lubrication of Steel–Aluminium Contact, *Nanomaterials*, 11(6), 1438 (2021). https://doi.org/10.3390/nano11061438

Roghani, H., Borhani, E., Ahmadi, E. and Jafarian, H. R., Study of changes in the aging process, microstructure, and mechanical properties of AA2024–AA1050 nanocomposites created by the accumulative roll bonding process, with the addition of 0.005 vol.% of alumina nanoparticles, *Discover Nano*, 19(1), 1 (2024). https://doi.org/10.1186/s11671-023-03917-2

Roghani, H., Borhani, E., Jafarian, H. R., Yousefieh, M., Naseri, M. and Ostovari, M. A., On the impact of using alumina nanoparticles and initial aging on the microstructure and mechanical properties of the AA1050/AA2024 nanostructure composite, created by accumulative roll bonding (ARB) method, *Wear*, 526, 204895 (2023). https://doi.org/10.1016/j.wear.2023.204895

Santhosh, K. K., Devaraju, A. and Manichandra, B., Investigating the Mechanical and Metallographic properties of FSWed dissimilar 6061 & 2024 Aluminum alloys by varying Distinctive Parameters, *Mater. Today Proc.*, 24880–886 (2020). https://doi.org/10.1016/j.matpr.2020.04.398

Slathia, S., Anand, R., Irfan, U. H. M., Raina, A., Mohan, S., Kumar, R. and Anand, A., Friction and Wear Behaviour of AA2024/ZrO2 Composites: Effect of Graphite, Recent Advances in Mechanical Engineering, *Springer*, 597–601 (2020). https://doi.org/10.1007/978-981-15-1071-7_49

Thiagarajan, C., Maridurai, T., Shaafi, T. and Muniappan, A., Machinability studies on hybrid nano-SiC and nano-ZrO2 reinforced aluminium hybrid composite by wire-cut electrical discharge machining, *Mater. Today Proc.*, 802731–2739 (2023). https://doi.org/10.1016/j.matpr.2021.07.029

Wei, P., Chen, Z., Yao, S., Huang, X., Li, B., Chen, Y., Huang, Z. and Lu, B., Enhancing strength and ductility of graphene and ZrO2 nanoparticles hybrid reinforced AA2024 composite fabricate by laser powder bed fusion, *Composites, Part A*, 185, 108378 (2024). https://doi.org/10.1016/j.compositesa.2024.108378